https://www.cytojournal.com/

CytoJournal

Editor-in-Chief:
Miaoqing Zhao, PhD., MD (Shandong First Medical University, Jinan, China)
He Wang, MD, PhD (Yale University School of Medicine, New Haven, Connecticut, USA)
Founding Editor & Editor-in-chief Emeritus:
Vinod B. Shidham, MD, FIAC, FRCPath (WSU School of Medicine, Detroit, USA)

OPEN ACCESS

Research Article

Zinc finger and broad-complex, tramtrack, and bric-a-brac domain containing 16 silencing attenuates bleomycin-induced pulmonary fibrosis in mice through inhibition of the phosphoinositide 3-kinase/protein kinase B/mammalian target of rapamycin pathway

Xiansong Fang, MS[1,2], Xiaoyun Wen, BS[3], Liang Zhou, BS[4], Yingjie Jiang, BS[4], Liefeng Wang, MD[2,5]*

[1]Department of Blood Transfusion, First Affiliated Hospital of Gannan Medical University, Ganzhou, [2]Department of Biochemistry and Molecular Biology, Gannan College of Medicine, China Medical University, Shenyang, [3]Department of Clinical Laboratory, First Affiliated Hospital of Gannan Medical University, Ganzhou, [4]The First School of Clinical Medicine, Gannan Medical University, Ganzhou, [5]School of Basic Medicine, Gannan Medical University, Ganzhou, China.

***Corresponding author:**

Liefeng Wang,
Department of Biochemistry and Molecular Biology, Gannan College of Medicine, China Medical University, Shenyang, School of Basic Medicine, Gannan Medical University, Ganzhou, China.

wlf0709@gmu.edu.cn.

Received: 04 November 2024
Accepted: 24 January 2025
Published: 01 April 2025

DOI
10.25259/Cytojournal_223_2024

Quick Response Code:

ABSTRACT

Objective: Idiopathic pulmonary fibrosis (PF) is a chronic and life-threatening lung disease. This study aimed to investigate the role of zinc finger and BTB domain containing 16 (Zbtb16), a transcription factor, in the progression of PF by analyzing its expression and regulatory effects in mouse and cell models.

Material and Methods: The gene expression profiles in bleomycin-induced (BL-I) PF lung tissues of mice were analyzed using the gene expression omnibus database. The mouse model of BL-I PF and cell model of transforming growth factor-β1 (TGF–β1)-induced mice lung epithelial cell (LEC) fibrosis was constructed. Zbtb16 expression was evaluated by reverse transcription quantitative polymerase chain reaction, Western blot, or immunohistochemistry. Tissue sections were assessed by hematoxylin and eosin, Masson, and terminal deoxynucleotidyl transferase dUTP nick-end labeling staining. The levels of protein, inflammation factors, and albumin were measured through Western blot or enzyme-linked immunosorbent assay.

Results: Bioinformatics analysis found that Zbtb16 was the highest differentially expressed marker in BL-I PF mice. Zbtb16 was highly expressed in the mice and cell model. Zbtb16 silencing could reduce lung tissues' collagen deposition, pulmonary edema, and pulmonary apoptotic cells; improve vascular permeability; and decrease fibrosis markers and inflammation factors expressed in model mice. Zbtb16 silencing could reduce fibrosis markers and inflammation factor levels in the cell model ($P < 0.05$). Kyoto encyclopedia of genes and genomes and gene set enrichment analyses suggested that Zbtb16 might regulate BL-I PF in mice through the phosphoinositide 3-kinases (PI3K)/protein kinase B (AKT)/mammalian target of rapamycin (mTOR) pathway (PAmT-P). Co-immunoprecipitation showed the combination of AKT and Zbtb16. PAmT-P in the mice model and cell model was visibly activated ($P < 0.05$), and Zbtb16 silencing could inhibit it ($P < 0.05$). Moreover, the rescue experiments showed that the AKT activator SC79 could reverse the effect of TGF-β1 + small interfere RNA-Zbtb16 on LECs.

Conclusion: This study identified Zbtb16 as a key regulator of PF progression, mediating its effects through the PAmT-P. Zbtb16 silencing alleviated fibrosis and inflammation *in vivo* and *in vitro*, providing a promising target for therapeutic intervention in PF.

Keywords: Bleomycin, Inflammation, Pulmonary fibrosis, Zinc finger and BTB domain containing 16

INTRODUCTION

Idiopathic pulmonary fibrosis (PF) is a chronic and life-threatening lung disease with a median survival of only about 3–5 years.[1,2] The clinical symptoms of patients with idiopathic PF primarily include decreased lung function and hypoxia accompanied by dyspnea during exercise or at rest. Its pathological features include abnormal accumulation of fibrous tissue within the lung parenchyma, replacement of healthy tissue with extracellular matrix (ECM), and destruction of the alveolar structure.[3] During PF, the damaged lung structure irreversibly and progressively impairs gas exchange, leading to hypoxic respiratory failure.[4] In the current clinical treatment, there is a deficiency of effective anti-PF drugs or strategies other than lung transplantation. In addition, the precise pathologic mechanisms of idiopathic PF remain largely unclear.[5] Thus, elucidating the underlying molecular mechanisms of idiopathic PF and developing new drugs or molecular targets that can delay or reverse the development of PF is imperative and crucial.

Zinc finger and BTB domain containing 16 (Zbtb16) belongs to the Zbtb family and is an evolutionarily conserved transcription factor mainly involved in immune response with metabolic regulation.[6,7] Moreover, Zbtb16 plays a key regulatory role in lung adenocarcinoma progression.[8] However, the potential effects of Zbtb16 on PF are limited. Growing pathogenesis research on PF has confirmed that alveolar epithelial injury triggers various inflammatory responses associated with PF, causing an increase in the release of pro-fibrotic mediators and disrupting the balance between pro-fibrotic and anti-fibrotic factors.[9] Myofibroblasts are crucial in promoting ECM deposition, releasing inflammatory mediators in response to epithelial injury, and they are the direct contributors to lung tissue degradation.[10] Recent studies have demonstrated that the phosphoinositide 3-kinase (PI3K)/protein kinase B (AKT)/mammalian target of rapamycin (mTOR) pathway (PAmT-P) is closely related to PF, and its insufficient activation and authoritarianism facilitate the onset of PF.[11] By enhancing AKT phosphorylation and activation, SC79 provides a valuable tool for evaluating the functional consequences of PAmT-P reactivation in fibrosis models. Nevertheless, whether Zbtb16 acts as a regulatory factor in the occurrence of the development of PF through PAmT-P remains to be studied.

The bleomycin-induced (BL-I) PF mice model is the most known animal model for the investigation of PF.[12] We processed and analyzed the chip data from GSE123293 and GSE43695 (representing wild-type control and BL-I PF mice, respectively) from the gene expression omnibus (GEO) database to screen differentially expressed genes in PF. The effect of Zbtb16 on the BL-I PF mice model and transforming growth factor-β1 (TGF-β1)-induced (T-β1-I) mice lung epithelial cell (LEC) model was evaluated *in vivo* and *in vitro*. The potential molecular regulatory mechanism of Zbtb16's involvement in the pathological process of PF through PAmT-P was verified.

MATERIAL AND METHODS

Microarray data processing

The gene expression profiles in wild-type control and BL-I PF lung tissues of mice were analyzed using raw data obtained from the National Center for Biotechnology Information GEO database (https://www.ncbi.nlm.nih.gov/geo/). Two conditions should be met for the screening of differentially expressed genes: |Fold change| ≥2 and $P < 0.05$. A heat map, volcano plot, and Venn diagram were constructed using the results of differentially expressed gene analysis. Kyoto Encyclopedia of Genes and Genomes (KEGG; https://www.genome.jp/kegg/) enrichment analysis was performed to evaluate the pathways associated with Zbtb16 in BL-I PF in mice.

BL-I PF model mice and sample collected

Twenty C57BL/6 male mice (6–8 weeks, 16–20 g) were purchased from GemPharmatech (Jiangsu, China). The mice were given free food and water in the specific pathogen-free laboratory, which was controlled at 23°C ± 2°C, relative humidity of 50% ± 10%, and light/dark cycle for 12 h. After adaptive feeding for 1 week, the mice were divided into four groups (5 per group): Control group, model group, model + short hairpin ribonucleic acid (shRNA)-negative control (NC) group, and model +shRNA-Zbtb16 group. The mice were anesthetized with 0.3% pentobarbital sodium (50 mg/kg) and injected with 50 μL of bleomycin (5 mg/kg; MedChemExpress) into the trachea to construct a PF model[13] (15, model group) or equivalent normal saline for control (5, control group). At 1 week post-modeling, the model mice with PF were injected with shRNA-NC lentivirus (5, shRNA-NC group) and shRNA-Zbtb16 lentivirus (5, shRNA-Zbtb16 group), both of which were procured from GenePharma. After 2 weeks of feeding, the mice were euthanized by injecting 0.3% pentobarbital sodium (150 mg/kg). The lungs of mice were isolated, and bronchoalveolar lavage fluid (BLF) was rapidly collected. BLF was obtained through tracheal intubation, washed 3 times with 300 μL of normal saline each time, and stored at −80°C. A portion of lung tissue was fixed with 4% paraformaldehyde and embedded in paraffin. The 5 μm-thick sections were used for hematoxylin and eosin (H&E), Masson, terminal deoxynucleotidyl transferase dUTP nick-end labeling (TUNEL) staining, and immunohistochemistry (IHC), and the remaining lung tissue was stored at −80°C for subsequent experiments.

Reverse transcription quantitative polymerase chain reaction (RT-qPCR)

Total ribonucleic acid (RNA) from lung tissues or cells was extracted using TRIzol reagent (15596018CN, Invitrogen, Thermo Fisher Scientific, MA, USA) and then reverse-transcribed into complementary deoxyribonucleic acid using PrimeScript RT Reagent Kit (RR037A, Takara, Shiga, Japan). Polymerase chain reaction (PCR) reactions were performed using SYBR Green PCR Master Mix (4368708, Applied Biosystems, Thermo Fisher Scientific) on an Applied Biosystems PCR system (Applied Biosystems). The primer sequences were as follows: Zbtb16 forward: 5'-TGGACTTCAGCACCTACGGG-3', reverse: 5'-CCGGAAGCTCGA CCCCACAC-3'. Glyceraldehyde-3-phosphate dehydrogenase (GAPDH) forward: 5'-GCTCATTTGCAGGGGGGAG-3', reverse: 5'-GTTGGTGGTGCAGGAGGCA-3'. Data were evaluated using the $2^{-\Delta\Delta CT}$ method and normalized to GAPDH.

IHC

After dewaxing and hydration, the lung sections were incubated overnight at 4°C with anti-Zbtb16 antibody (LS-C334349-20, Vector Laboratories, CA, USA). After washing, they were incubated at 25°C for 1 h with goat-anti mouse secondary antibody (1:1000, ab205719, Abcam). The sections were then stained using a 3,3'-diaminobenzidine (DAB) staining kit (ZLI-9019, Zhongshan Jinqiao Biotechnology, Beijing, China) according to the reagent instructions. Finally, the distribution of Zbtb16 protein was observed under a microscope (CKX41, Olympus, Tokyo, Japan). Brown particles in the cells were considered positive, and their area was analyzed using ImageJ software (National Institutes of Health [NIH], USA).

H&E and Masson staining

After dewaxing and hydration, the lung sections were stained using an H&E kit (G1120, Solarbio, Beijing, China) or Masson staining kit (G1340, Solarbio) according to the reagent instructions. The sections were stained and observed under a microscope (Olympus). Inflammatory infiltrated areas and percentage of collagen deposition were determined using ImageJ software.

TUNEL staining

The lung sections were stained using a TUNEL staining kit according to the reagent instructions (KGA1400, KeyGen Biotech, Jiangsu, China). The paraffin-embedded lung tissue sections were dewaxed in fresh xylene, hydrated with anhydrous ethanol, 90% ethanol, 70% ethanol, and distilled water, and incubated with protease K solution. TUNEL detection solution was added, with staining conducted at 37°C for 1 h in the dark to prevent dye volatilization. After washing, the samples were stained with DAB and subjected to re-staining with hematoxylin. The stained samples were observed under a microscope (CKX41, Olympus) and photographed. Tunnel-positive cell areas were analyzed using ImageJ software.

Wet/dry weight ratio of mouse lung tissue

After the lungs of mice were excised, a segment of the lung tissue was obtained to absorb the blood on the lung surface and then weighed (wet weight). The lung tissue was placed in an oven (DHG-9140A, Huitai instrument, Shanghai, China) at 80°C for 48 h and weighed (dry weight) using an electronic balance (GL2202-1SCN, Huruiming, Guangzhou, China). The wet weight/dry weight ratio was calculated.[14]

Cell culture and treatment

Mouse LEC line MLE-12 was obtained from Shanghai Kanglang shengwu (KL036M, Shanghai, China), which underwent short tandem repeat and mycoplasma testing. Cells were cultured in Dulbecco's modified eagle medium (11965118, DMEM, Gibco, Thermo Fisher Scientific) supplemented with 10% fetal bovine serum (A5670701, Invitrogen) and 100 μg/mL streptomycin + 100 U/mL penicillin (15140122, Gibco). The cells were incubated at 37°C containing 5% CO_2. To simulate cell fibrosis,[15] we treated the cells with 10 ng/mL TGF-β1 (H8541, Sigma-Aldrich, MO, USA) for 24 h. In experiments with SC79, we administered SC79 (10 μmol/L; AKT activator, 123871-25MG, Sigma-Aldrich) and TGF-β1 to the cells for stimulation. Both small interfere RNA (siRNAs) targeting Zbtb16 (si-Zbtb16) and its negative control (si-NC) were purchased from GenePharma (Shanghai, China). The si-Zbtb16 sequence was 5'-CTGCAGTTAGAAGAGAATATT-3', and the si-NC sequence was 5'-GCTGCTTTGGACAAGGCUATT-3'. Cell transfection was carried out using Lipofectamine 2000 reagent (11668500, Invitrogen) according to the manufacturer's protocol. In brief, small interfere RNA siRNA and Lipofectamine 2000 were diluted in Opti-Minimum essential medium (31985070, Gibco) separately and then mixed for 5 min at 21°C. The mixture was added dropwise to cells in antibiotic-free DMEM, and the medium was replaced with complete DMEM after 6 h. Cells were harvested 48 h post-transfection for subsequent experiments.

Western blot and co-immunoprecipitation (Co-IP)

Cells were collected from tissues and lysed in radio-immunoprecipitation assay buffer (P0013D, Beyotime, Shanghai, China) containing protease and phosphatase inhibitor (P1046, Beyotime). The denatured protein sample (30 μg) was electrophoretically separated on sodium dodecyl sulfate polyacrylamide gel electrophoresis gels (P1200,

Solarbio) and transferred to a polyvinylidene fluoride membrane (3010040001, Millipore, MA, USA). After blocking with 5% skimmed milk, the blots were incubated overnight at 4°C with the anti-Immunoglobulin G (IgG) (#5873, Cell Signaling Technology, MA, USA) or primary antibodies: anti-Zbtb16 antibody (1:1000, ab104854, Abcam, Cambridge, UK), anti-collagen I antibody (1:1000, ab270993, Abcam), anti-fibronectin (Fn) antibody (1:1000, ab2413, Abcam), anti-a-smooth muscle actin (SMA) antibody (1:1000, ab7817, Abcam), or anti-GAPDH antibody (1:1,500, ab181602, Abcam). After rinsing, the membranes were incubated with the horseradish peroxidase-labeled secondary antibody (1:1500, ab205718, or ab6728, Abcam) for 2 h at 25°C and then washed. The protein bands were assessed using an ECL developer (Thermo Fisher Scientific), and Image J software (version 1.45, NIH, USA) was used to analyze the grayscale values. For Co-IP, cell lysates were mixed with Zbtb16 antibody or IgG and incubated at 4°C for 12 h. Thereafter, 5 μL of protein A and 5 μL of protein G were added, and the mixture was gently mixed at 4°C for 3 h. The sample was then centrifuged at 12,000 g for 1 min, and the precipitate was retained for Western blot analysis to measure Zbtb16 and AKT protein levels.

Enzyme-linked immunosorbent assay (ELISA)

The levels of interleukin (IL)-1β (CME0015-F), IL-6 (CME0006-F), and tumor necrosis factor (TNF)-α (CME0004-F) in BLF or cell culture medium supernatant were assessed using ELISA detection kits in accordance with the protocol of the manufacturer (Sizhengbai Biotechnology, Jiangsu, China).

Statistical analysis

The data were analyzed using Statistical Package for the Social Sciences 22.0 (IBM, NY, USA). All values were presented as means ± Standard deviation. Statistical differences were assessed using *t*-test (for two groups) or one-way analysis of variance (for diverse groups) followed by Bonferroni *post hoc* analysis. The statistical deviation was determined at $P < 0.05$.

RESULTS

Zbtb16 was markedly elevated in BL-I PF lungs of mice

To screen out the aberrantly expressed genes in the BL-I PF lung tissues of mice, we initially selected the sequencing data from the wild-type control and BL-I PF lung tissues of mice in the GEO database. Subsequently, two datasets, GSE123293 and GSE43695, were selected, and the differentially expressed genes in these two datasets were analyzed [Figure 1a and b]. Using Venn diagrams, we observed that 39 and 26 differentially expressed genes were simultaneously downregulated [Figure 1c] or upregulated [Figure 1d], respectively, in the two datasets. The overlap of highly expressed differential genes in the GSE123293 and GSE43695 datasets is shown in Figure 1e. These results confirmed that Zbtb16 had the largest differential expression in the BL-I PF lung tissues of mice.

Zbtb16 silencing mitigated BL-I PF and inflammation in mice

To explore the role of Zbtb16 in BL-I PF mice, we first constructed Zbtb16-silenced lentivirus (shRNA-Zbtb16) and shRNA-NC. One week after modeling the mice with PF, the shRNA-NC lentivirus and shRNA-Zbtb16 lentivirus were injected into the trachea. After 2 weeks of feeding, the lung tissue and BLF were collected. The lung tissues were analyzed by RT-qPCR and Western blot, which revealed that the expression levels of Zbtb16 messenger RNA (mRNA) and protein were markedly increased in the model mice group, whereas shRNA-Zbtb16 lentivirus injection could visibly decrease Zbtb16 expression in lung tissue of the model mice group ($P < 0.01$) [Figure 2a and b].

Zbtb16 silencing reduces inflammation, collagen deposition, and apoptosis in lung tissue

IHC results showed that Zbtb16 expression in the model mice group was visibly higher than that in the control group ($P < 0.001$); Zbtb16 silencing could visibly reduce Zbtb16 expression ($P < 0.001$) [Figure 3a]. H&E staining showed that the alveolar septum in the model group was thicker than that in the control group, and inflammatory cell infiltration could be observed ($P < 0.001$). After treatment with sh-Zbtb16 lentivirus, the alveolar spacing in lung tissues of the model +shRNA-Zbtb16 group mice diminished, and the infiltration of inflammatory cells in lung tissues also decreased ($P < 0.001$) [Figure 3b]. Masson staining showed that the lung tissue of the control group was normal without obvious staining, whereas the lung tissue of the model group exhibited collagen fiber deposition, indicated by blue staining ($P < 0.001$). After treatment with shRNA-Zbtb16 lentivirus, the collagen fiber deposition and blue staining in lung tissues of the model group +shRNA-Zbtb16 mice decreased ($P < 0.01$) [Figure 3c]. TUNEL staining showed that the number of apoptotic lung cells in the model group was visibly higher than that of the control group ($P < 0.001$), and the number of apoptotic lung cells in the model +shRNA-Zbtb16 group mice was visibly reduced after treatment with shRNA-Zbtb16 lentivirus ($P < 0.001$) [Figure 3d].

Zbtb16 silencing alleviates lung edema, reduces fibrosis markers, and decreases inflammatory cytokines

The wet/dry ratio of lung tissue in the model group was higher than that in the control group ($P < 0.01$), whereas the

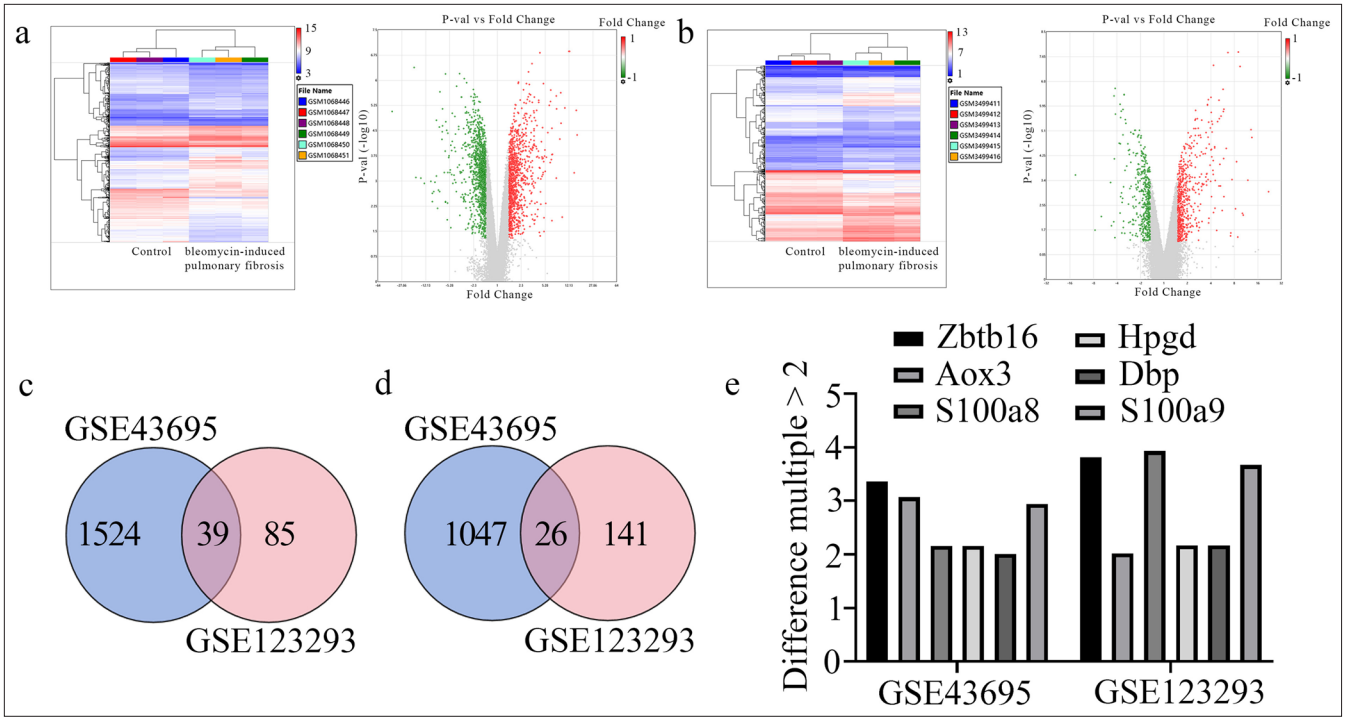

Figure 1: Bioinformatics analysis and screening of differentially expressed genes between wild-type control and BL-I PF lung tissues of mice in the gene expression omnibus database. (a) The heat map and volcano plot of differentiating genes in the GSE43695 dataset. (b) The heat map and volcano plot of differentiating genes in the GSE123293 dataset. (c) The Venn diagram illustrating the intersection of low-expression differential genes in the GSE123293 and GSE43695 datasets. (d) The Venn diagram illustrating the intersection of high-expression differential genes in the GSE123293 and GSE43695 datasets. (e) Intersection of highly expressed distinguishing genes in the GSE123293 and GSE43695 datasets (difference multiple >2). Zbtb16: Zinc finger and BTB domain containing 16, HPGD: 15-hydroxyprostaglandin dehydrogenase, AOX3: Aldehyde oxidase 3, DBP: D-box binding PAR BZIP transcription factor, S100A8: S100 calcium binding protein A8, S100A9: S100 calcium binding protein A9, BL-I: Bleomycin-induced, PF: Pulmonary fibrosis.

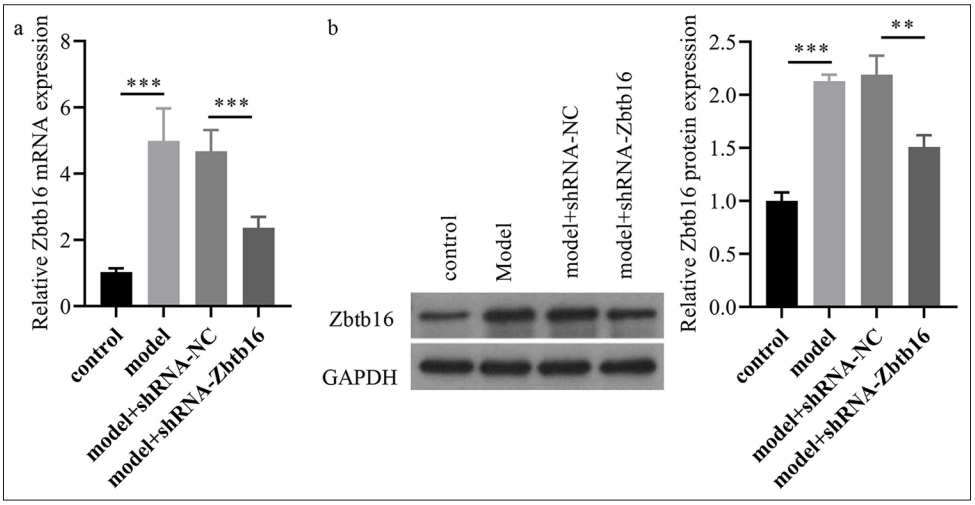

Figure 2: Zbtb16 silencing mitigated BL-I PF and inflammation in mice. (a and b) The Zbtb16 mRNA and protein expression levels in lung tissues of mice were measured via qRT-PCR and Western blot. $n = 3$; $^{**}P < 0.01$; $^{***}P < 0.001$. Zbtb16: Zinc finger and BTB domain containing 16, NC: Negative control, BL-I: Bleomycin-induced, RT-qPCR: Reverse transcription quantitative polymerase chain reaction, PF: Pulmonary fibrosis.

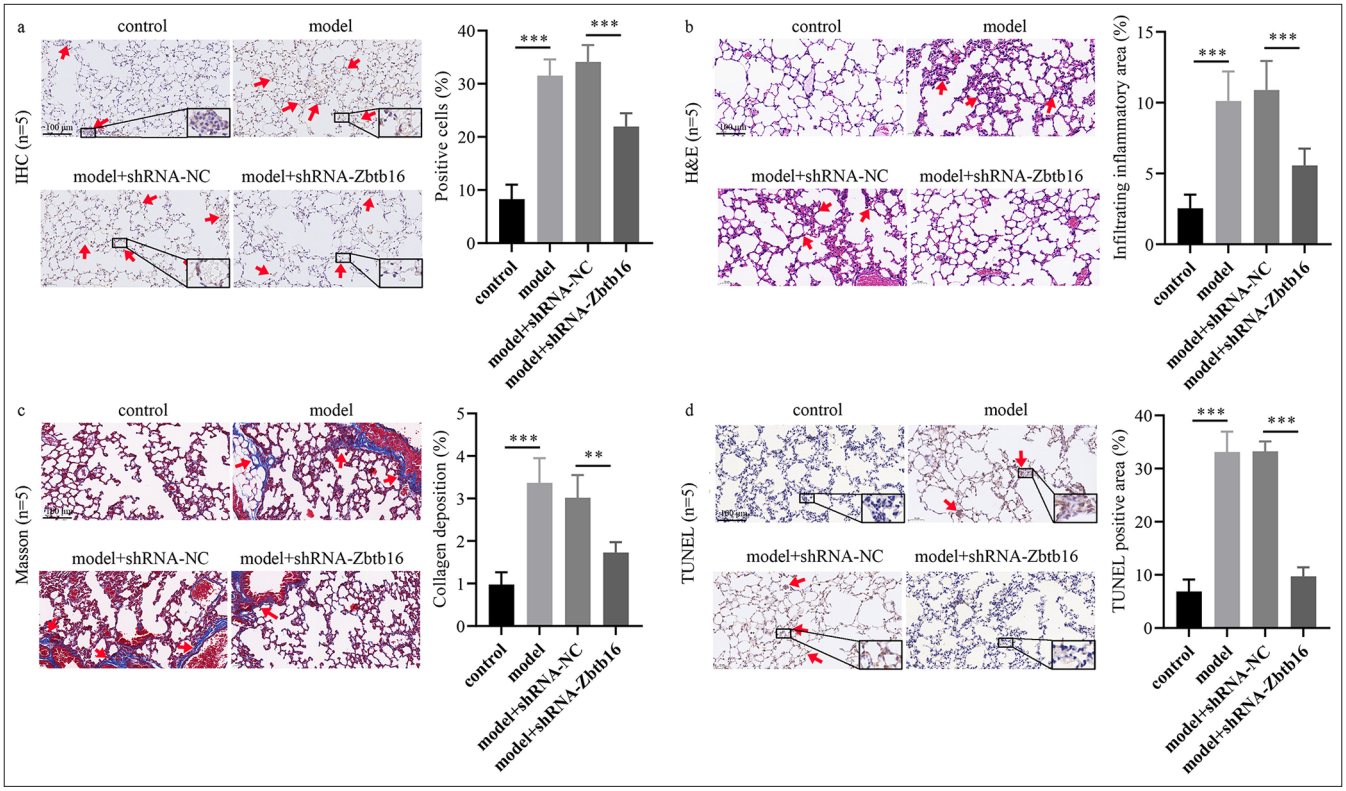

Figure 3: Zbtb16 silencing mitigated BL-I PF and inflammation in mice. (a) Lung tissue sections were stained with anti-Zbtb16 antibody by IHC to evaluate Zbtb16 protein expression. The red arrows indicate Zbtb16 protein-positive expression in this region of the tissue. (magnification: 100x) (b) Lung tissue sections were stained with H&E to examine alveolar structure and inflammatory cell infiltration. The red arrows indicate extensive inflammatory infiltration in this region of the tissue. (magnification: 100x) (c) Lung tissue sections were stained with Masson's trichrome to evaluate collagen fiber deposition. The red arrows indicate significant collagen fiber deposition in this region of the tissue. (magnification: 100) (d) Lung tissue sections were subjected to TUNEL staining to assess apoptotic cell levels. The red arrows indicate a prominent aggregation of TUNEL-positive cells in this region of the tissue. (magnification: 100x) $n = 5$; $^{**}P < 0.01$; $^{***}P < 0.001$. Zbtb16: Zinc finger and BTB domain containing 16, NC: Negative control, IHC: Immunohistochemical, H&E: Hematoxylin and eosin, BL-I: Bleomycin-induced, TUNEL: Terminal deoxynucleotidyl transferase dUTP nick-end labeling, PF: Pulmonary fibrosis.

wet/dry ratio of lung tissue in the model +shRNA-Zbtb16 group was lower than that in the model +shRNA-NC group ($P < 0.05$) [Figure 4a]. The concentration of albumin in BLF of the model group was higher than that in the control group ($P < 0.001$), whereas the concentration of albumin in BLF of the model +shRNA-Zbtb16 group was lower than that in the model +shRNA-NC group ($P < 0.001$) [Figure 4b]. Western blot showed that the protein levels of myofibroblast markers (collagen I and Fn with α-SMA) in lung tissues of the model group mice visibly increased compared with that in the control group, and the protein levels of myofibroblast markers in lung tissues of the model +shRNA-Zbtb16 group mice visibly decreased compared with those in the model +shRNA-NC group ($P < 0.01$) [Figure 4c and d]. ELISA results showed that the levels of inflammatory factors (TNF-α and IL-6 with IL-1β) in BLF of the model group mice visibly increased compared with that in the control group, and the levels of inflammatory factors in BLF of the model +shRNA-Zbtb16 group mice visibly decreased compared with that in the model +shRNA-NC group ($P < 0.001$) [Figure 4e].

Zbtb16 silencing alleviated T-β1-I mice LEC fibrosis and inflammation

This study used the T-β1-I mice LEC model to investigate the regulatory role of Zbtb16 in mice LEC fibrosis. Subsequently, si-Zbtb16 was transfected to silence Zbtb16 expression in cells, and the effect of Zbtb16 silencing on fibrosis and inflammation T-β1-I mice LECs was verified. As expected, Zbtb16 mRNA and protein expression levels visibly increased in the T-β1-I LEC group, whereas transfection with si-Zbtb16 decreased Zbtb16 mRNA ($P < 0.001$) and protein expression levels ($P < 0.05$) in the TGF-β1+ si-Zbtb16 group [Figure 5a and b]. The protein expression of myofibroblast markers visibly increased in the T-β1-I LEC group, whereas the protein expression of myofibroblast markers decreased in

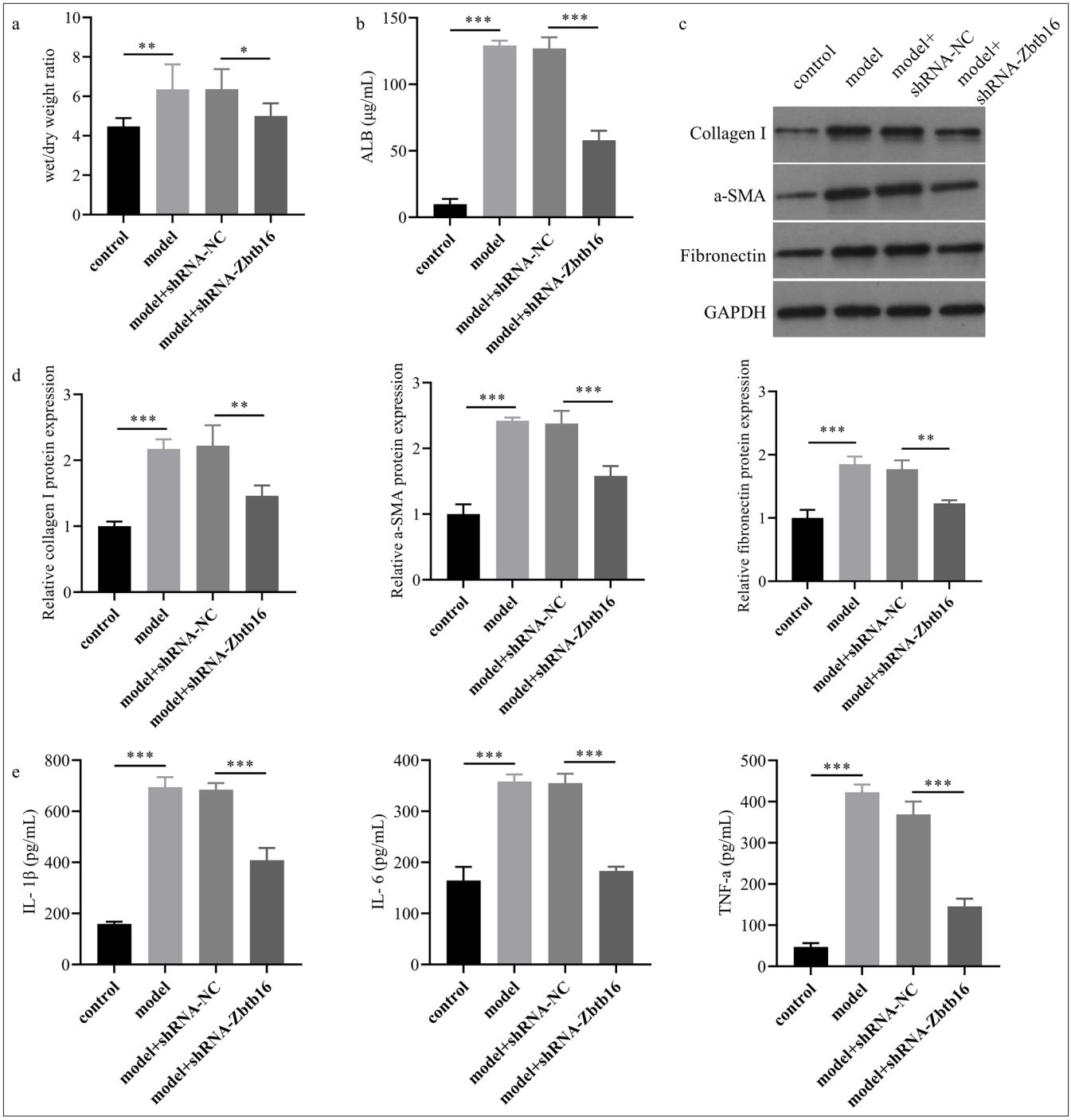

Figure 4: Zbtb16 silencing mitigated BL-I PF and inflammation in mice. (a) The wet/dry ratio of lung tissue was measured. (b) The albumin concentration in BLF of mice lung was assessed by ELISA. (c and d) The protein levels of collagen I, Fn, and α-SMA in lung tissues of mice were assessed by Western blot. (e) The levels of inflammatory factors TNF-α, IL-6, and IL-1β in BLF of mice lung were assessed by ELISA. $n = 3$; *$P < 0.05$; **$P < 0.01$; ***$P < 0.001$. Zbtb16: Zinc finger and BTB domain containing 16, NC: Negative control, TNF-α: Tumor necrosis factor-α, IL-6: Interleukin 6, IL-1β: interleukin 1β, Fn: Fibronectin, α-SMA: α-smooth muscle actin, ALB: Albumin; ELISA: Enzyme-linked immunosorbent assay, Fn: Fibronectin, BLF: Bronchoalveolar lavage fluid, PF: Pulmonary fibrosis.

the TGF-β1+ si-Zbtb16 group ($P < 0.01$) [Figure 5c and d]. The levels of inflammatory factors visibly increased in the culture medium supernatant of the T-β1-I LEC group, whereas the levels of inflammatory factors decreased in the culture medium supernatant of the TGF-β1+ si-Zbtb16 group ($P < 0.001$) [Figure 5e].

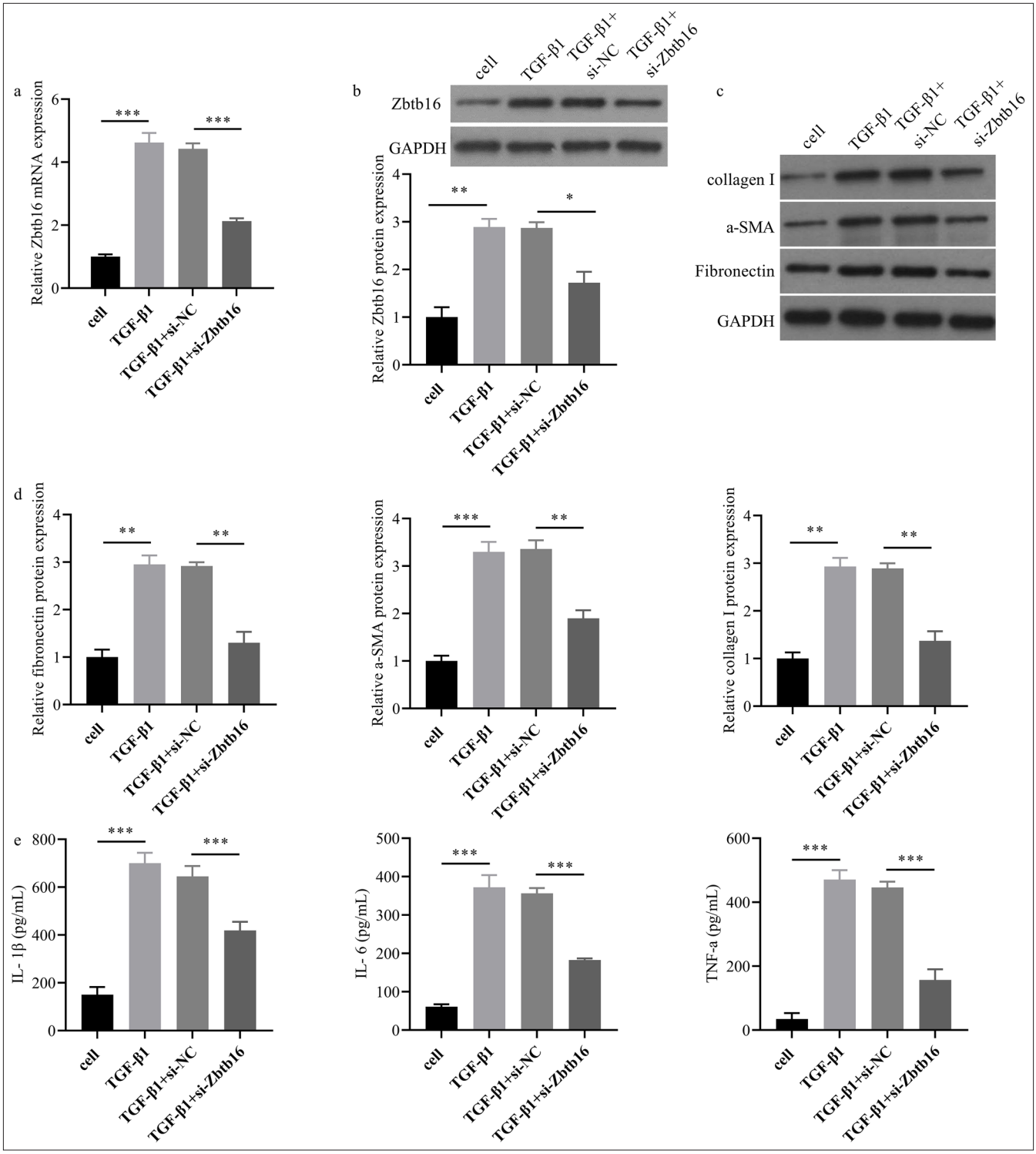

Figure 5: Zbtb16 silencing alleviated T-β1-I mice LEC fibroblasts and inflammation. (a and b) The Zbtb16 mRNA and protein expression levels in mice LECs were measured by qRT-PCR and Western blot. (c and d) The protein levels of collagen I, Fn, and α-SMA in mice LECs were assessed by Western blot. (e) The levels of inflammatory factors TNF-α, IL-6, and IL-1β in cell culture medium supernatant were assessed by ELISA. $n = 3$; *$P < 0.05$; **$P < 0.01$; ***$P < 0.001$. Zbtb16: Zinc finger and BTB domain containing 16, NC: Negative control, TNF-α: Tumor necrosis factor-α, IL-6: Interleukin 6, IL-1β: Interleukin 1β, Fn: Fibronectin, α-SMA: α-smooth muscle actin, ALB: Albumin, ELISA: Enzyme-linked immunosorbent assay, Fn: Fibronectin, LEC: Lung epithelial cell.

Bioinformatics predicted that Zbtb16 might be involved in BL-I PF of mice

The above animal and cell experiments confirmed that Zbtb16 silencing could alleviate BL-I PF in mice and T-β1-I mice LEC fibrosis. However, the specific mechanism of action remains unclear. Thus, by mining the data in GEO, KEGG, and gene set enrichment analysis (GESA) predicted that Zbtb16 might be involved in BL-I PF in mice. KEGG and GESA predicted that Zbtb16 might regulate BL-I PF in mice through PAmT-P [Figure 6a and b]. CO-IP showed the combination of AKT and Zbtb16 ($P < 0.001$) [Figure 6c]. The Western blot results showed that p-AKT and p-mTOR in BL-I PF lung tissues of mice and T-β1-I fibrosis mice LECs were visibly higher than those in the control group, whereas Zbtb16 silencing could inhibit BL-I and T-β1-I PAmT-P activation and reverse the rise in p-AKT/AKT and p-mTOR/mTOR levels. However, the total expression of AKT and mTOR did not change ($P < 0.05$) [Figure 6d-f].

Zbtb16 silencing alleviated T-*β*1-I mice LEC fibrosis by blocking PAmT-P

Subsequently, we investigated whether the protective effect of Zbtb16 silencing on PF was achieved by inhibiting PAmT-P. si-Zbtb16 was transfected into T-β1-I mice LECs, and p-AKT activator (10 μmol/L SC79) was added. Rescue experiments showed that adding SC79 into TGF-β1 + si-Zbtb16 cells could increase the levels of p-AKT/AKT and p-mTOR/mTOR and reactivate PAmT-P ($P < 0.001$) [Figure 7a]. SC79 could reverse the effect of TGF-β1 + si-Zbtb16 on mice LECs and increase the expression of myofibroblast markers in TGF-β1 + si-Zbtb16 cells and inflammatory factors in cell culture medium supernatant ($P < 0.05$) [Figures 7b and c].

DISCUSSION

PF is a chronic and destructive disease that leads to reduced quality of life and shortened life expectancy due to limited treatment options at present.[16,17] Therefore, the pathological progression of PF necessitates the identification of novel targeted markers or treatment strategies. Here, we utilized bioinformatics to predict and confirm that ZBTB16 was markedly elevated in a mouse model of BL-I PF and in a cell model of T-β1-I mice LEC fibrosis. Zbtb16 silencing in lung tissues of the BL-I PF mouse model could alleviate lung collagen deposition, pulmonary edema, and pulmonary vascular permeability, reduce the rate of cell apoptosis, and decrease the expression levels of fibrotic markers and inflammatory factors. In the T-β1-I mice LEC model, Zbtb16 silencing could reduce the levels of fibrosis markers and inflammatory factors. Interestingly, we found that PAmT-P in the BL-I PF mice model group and T-β1-I LEC model group was visibly activated, whereas Zbtb16 silencing could inhibit PAmT-P activation in the mouse and cell models. Moreover, the rescue experiments verified that the AKT activator SC79 could reverse the effect of TGF-β1 + si-Zbtb16 on mice LECs. These results provide theoretical evidence that Zbtb16 silencing attenuated BL-I PF in mice by inhibiting PAmT-P.

Zbtb16 functions as a transcription factor that can act as a transcriptional inhibitor and activator, regulating many biological processes. Zbtb16 may regulate the susceptibility of T2DM mice to atrial fibrillation through the Txnip–Trx2 pathway.[18] In renal interstitial fibrosis, Song *et al*.[19] reported that treatment of HEK293 cells with renin induces Zbtb16 nuclear translocation, which then binds to the promoter of the PRR gene, thereby inhibiting PRR transcription and other markers of renal interstitial fibrosis expression; Zbtb16 knockdown had the opposite effect. However, the potential effect of Zbtb16 on PF remains unclear. Here, we analyzed the GSE123293 and GSE43695 datasets (wild-type control and BL-I PF lung tissues of mice) through bioinformatics, screened differentially expressed genes, and found that Zbtb16 had the highest expression and largest difference. Bleomycin could induce PF and pulmonary inflammation within a short time. Thus, the PF model constructed by intratracheal injection of bleomycin is an important model for investigating the pathological progression of PF and identifying novel therapeutic agents.[20] Here, the PF mouse model of BL-I was constructed. We observed the significant expression of mRNA and protein of Zbtb16 in lung tissues of the BL-I PF mice model. The pathological detection of mice model lung tissues revealed obvious PF and inflammatory characteristics. Surprisingly, Zbtb16 silencing in the lungs of the BL-I PF mice model suggested pathological changes in lung tissues. Zbtb16 silencing decreased collagen deposition in lung tissues, the rate of cell apoptosis, pulmonary edema, and pulmonary vascular permeability. The increased expression of collagen I and Fn served as an indicator of PF occurrence, whereas α-SMA suggested fibroblast activation; the increased level resulted in the transformation of fibroblasts into myofibroblasts, initiating PF development.[11] In PF model mice lung tissues, the expression of collagen I, Fn, and α-SMA proteins markedly increased, whereas Zbtb16 silencing could reduce the expression levels of collagen I, Fn, and α-SMA protein. We also assessed the levels of the inflammatory cytokines TNF-α, IL-6, and IL-1β in the BLF of mice, and we found that Zbtb16 silencing could reduce their expression levels. TGF-β1 activates lung fibroblasts and accelerates the process of trans-differentiation.[21] We conducted simultaneous TGF-β1 tests on mice LECs to construct a PF cell model. Similar to the animal model of PF *in vivo*, the levels of Zbtb16 expression, fibrosis marker collagen I, Fn, α-SMA, and inflammatory factors TNF-α, IL-6, and IL-1β in the PF cell model increased; Zbtb16 silencing in PF model cells could reduce levels of fibrosis markers and inflammatory factors.

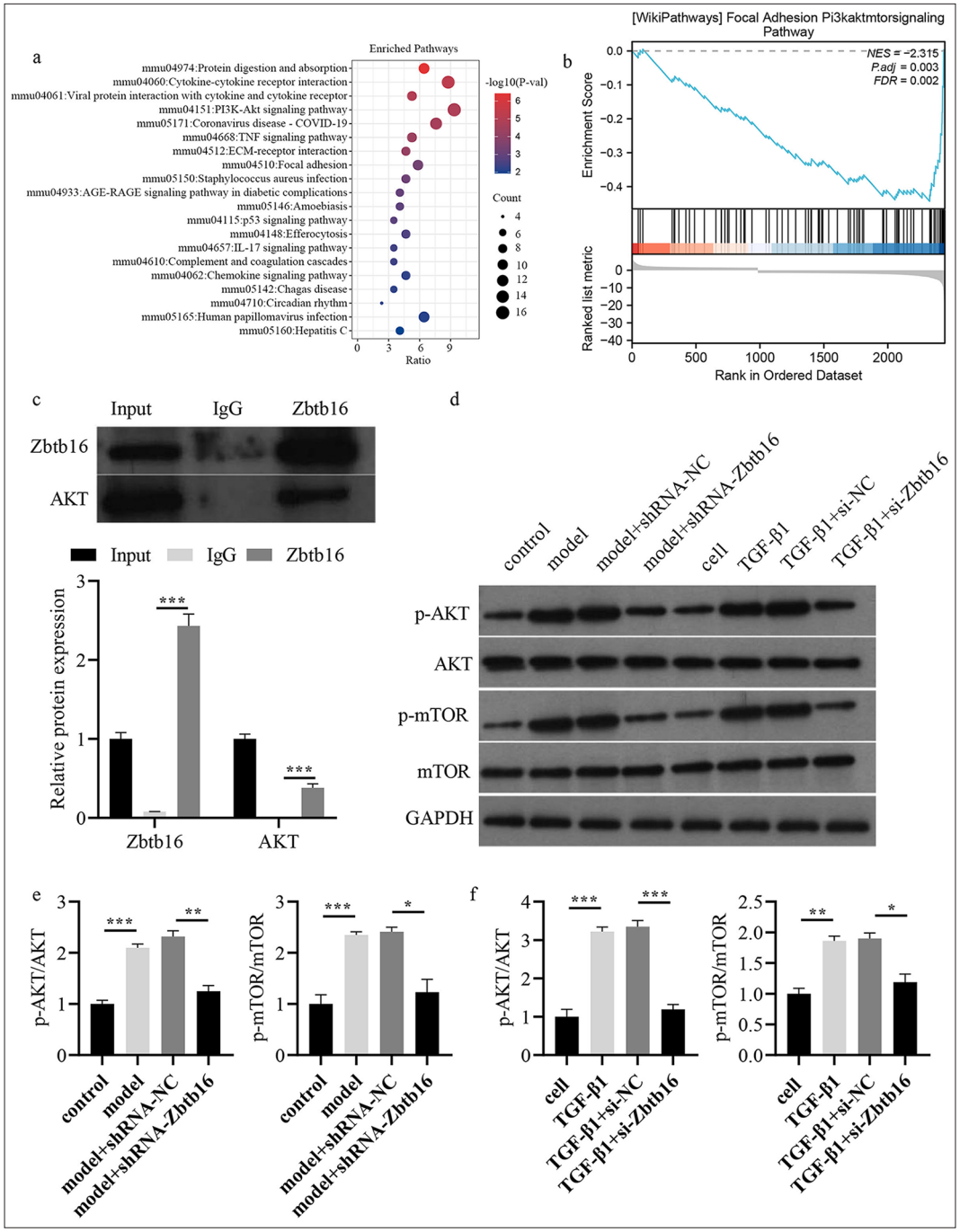

Figure 6: Bioinformatics predicted that Zbtb16 might be involved in BL-I PF of mice. (a) KEGG analysis predicted that Zbtb16 might be involved. (b) GESA analysis predicted that PAmT-P of Zbtb16 might be involved. (c) CO-IP was used to analyze the combination of AKT and Zbtb16. (d) The PAmT-P-related protein expression levels in mice lung tissues and mice LECs were measured by Western blot. (e) p-AKT/AKT and p-mTOR/mTOR levels were shown in BL-I PF lung tissues of mice; (f) p-AKT/AKT and p-mTOR/mTOR levels were shown in T-β1-I fibrosis mice LECs. $n = 3$; *$P < 0.05$; **$P < 0.01$, ***$P < 0.001$. Zbtb16: Zinc finger and BTB domain containing 16, NC: Negative control, AKT: Protein kinase B, p-AKT: Phosphorylated AKT, mTOR: Mammalian target of rapamycin, p-mTOR: Phosphorylated mTOR, TNF-α: Tumor necrosis factor-α, IL-6: Interleukin 6, IL-1β: Interleukin 1β, Fn: Fibronectin, α-SMA: α-smooth muscle actin, ALB: Albumin, ELISA: Enzyme-linked immunosorbent assay, LEC: Lung epithelial cell, BL-I: Bleomycin-induced, GESA: Gene set enrichment analysis, KEGG: Kyoto encyclopedia of genes and genomes, PAmT-P: PI3K/AKT/mTOR pathway, PF: Pulmonary fibrosis.

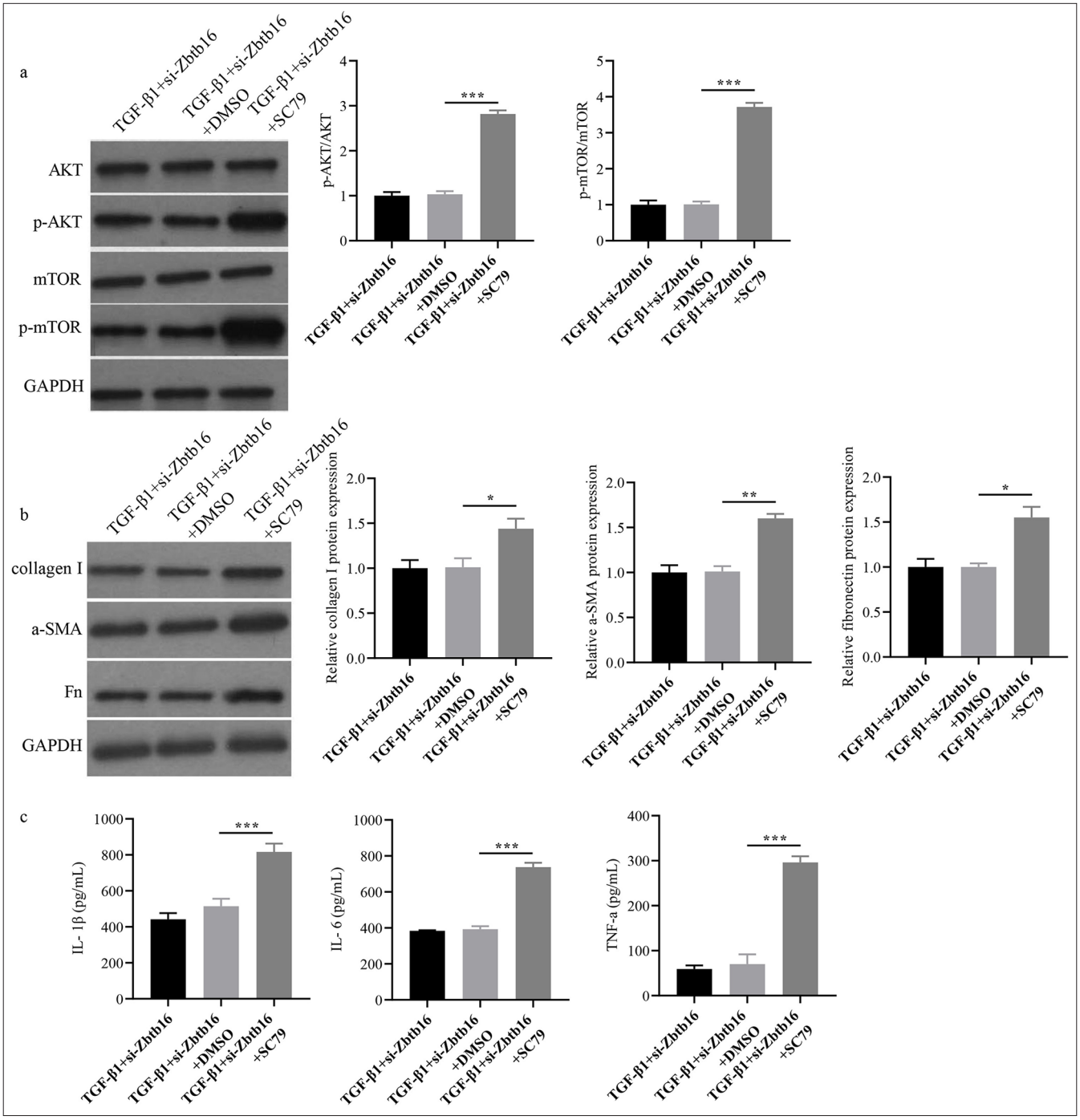

Figure 7: Zbtb16 silencing alleviated T-β1-I mice LEC fibrosis by blocking PAmT-P. (a and b) The PAmT-P-related protein and collagen I, Fn, and α-SMA protein expression levels in mice LECs were measured through Western blot. (c) The TNF-α, IL-6, and IL-1β concentrations in mice LEC culture medium supernatant were detected by ELISA. $n = 3$; *$P < 0.05$; **$P < 0.01$; ***$P < 0.001$. Zbtb16: Zinc finger and BTB domain containing 16, NC: Negative control, AKT: Protein kinase B, p-AKT: Phosphorylated AKT, mTOR: Mammalian target of rapamycin, p-mTOR: Phosphorylated mTOR, PAmT-P: PI3K/AKT/mTOR pathway, Fn: Fibronectin, α-SMA: α-smooth muscle actin, LEC: Lung epithelial cell, TNF-α: Tumor necrosis factor-α, IL-6: Interleukin 6, IL-1β: Interleukin 1β, ELISA: Enzyme-linked immunosorbent assay.

To understand the protective mechanism of Zbtb16 silencing on BL-I PF mice and T-β1-I mice LECs, we mined the data in GEO. KEGG and GESA predicted that Zbtb16 might regulate BL-I PF in mice through PAmT-P. PAmT-P is the main

pathway that mediates cell survival by inhibiting apoptosis and stimulating cell proliferation.[22] Previous studies have confirmed that PAmT-P is closely related to the development of PF.[23,24] Activation of PAmT-P can reduce autophagy, increase the apoptosis of alveolar epithelial cells, promote the expression of fibrosis markers, α-SMA expression, and EMT, and accelerate fibrosis.[25,26] Here, we assessed the expression of PAmT-P-related proteins in BL-I PF mice and T-β1-I mice LECs, and we found that PAmT-P in the BL-I PF mice model and T-β1-I LEC model was visibly activated. By contrast, Zbtb16 silencing could block PAmT-P in the BL-I PF mice model and T-β1-I LEC model. The results depicted in Figures 5 and 6 further illustrate the functional relationship between Zbtb16 silencing and PAmT-P pathway inhibition. Specifically, the reduction in p-AKT and p-mTOR levels in Zbtb16-silenced models highlights the direct impact of this pathway on fibrosis progression. Moreover, the rescue experiments with SC79, which partially restored fibrosis markers and inflammatory cytokines, provided additional evidence supporting the regulatory role of PAmT-P in Zbtb16-mediated attenuation of fibrosis and inflammation. These findings underscore the central role of this pathway in mediating the protective effects of Zbtb16 silencing. SC79 could reverse the effect of TGF-β1+si-Zbtb16 on mice LECs and increase the levels of fibrosis marker collagen I, Fn, α-SMA, and inflammatory factors. All the above results indicated that Zbtb16 silencing protected BL-I PF in mice by inhibiting PAmT-P.

This study had certain limitations. First, it did not address the association between Zbtb16 expression and clinical characteristics in patient-derived samples. Second, although numerous signaling pathways are involved in the progression of PF, this study focused exclusively on the role of the PAmT-P, particularly in the context of Zbtb16 silencing. Finally, the upstream signals regulating Zbtb16 expression and its potential mechanisms were not thoroughly investigated. These limitations represent key directions and objectives for future research.

SUMMARY

Our research declared that ZBTB16 was dramatically elevated in the mouse model of BL-I PF and cell model of T-β1-I LEC fibrosis. Zbtb16 silencing mitigated BL-I PF in mice by inhibiting PAmT-P. Zbtb16 might be a promising biomarker for PF potential or adjuvant treatment in the future.

AVAILABILITY OF DATA AND MATERIALS

The datasets and materials used and/or analyzed during the present study are available from the corresponding author on reasonable request.

ABBREVIATIONS

BLF: Bronchoalveolar lavage fluid
BL-I: Bleomycin-induced
Co-IP: Co-immunoprecipitation
DMEM: Dulbecco's modified eagle medium
ECM: Extracellular matrix
ELISA: Enzyme-linked immunosorbent assay
Fn: Fibronectin
GEO: Gene expression omnibus
GESA: Gene set enrichment analysis
H&E: Hematoxylin and eosin
IHC: Immunohistochemistry
IL: Interleukin 6
KEGG: Kyoto encyclopedia of genes and genomes
LECs: Lung epithelial cells
mTOR: Mammalian target of rapamycin
NC: Negative control
p-AKT: Phosphorylated AKT
PAmT-P: PI3K/AKT/mTOR pathway
PF: Pulmonary fibrosis
p-mTOR: Phosphorylated mTOR
RT-qPCR: Reverse transcription quantitative polymerase chain reaction
SPF: Specific pathogen-free
TNF-α: Tumor necrosis factor-α
TUNEL: Terminal deoxynucleotidyl transferase dUTP nick-end labeling
T-β1-I: TGF-β1-induced
Zbtb16: Zinc finger and BTB domain containing 16
α-SMA: α-Smooth muscle actin

AUTHOR CONTRIBUTIONS

LFW: Designed the study, supervised the experiments, and participated in drafting and critically revising the manuscript for important intellectual content; XSF and XYW: Conducted the experiments and collected data; LZ: Performed data analysis and contributed to the interpretation of results; YJJ: Assisted with drafting the manuscript and prepared figures. All authors contributed to the critical revision of the manuscript for important intellectual content, gave final approval of the version to be published, participated fully in the work, and take public responsibility for appropriate portions of the content. All authors agree to be accountable for all aspects of the work, ensuring that questions related to the accuracy or completeness of any part of the work are appropriately investigated and resolved.

ETHICS APPROVAL AND CONSENT TO PARTICIPATE

This study has been approved by the Ethics Committee of the First Affiliated Hospital of Gannan Medical

University, approval number No. LLSC-2024-252, dated September 3, 2024. This article does not involve patients, so informed consent is not required.

ACKNOWLEDGMENTS

Not applicable.

FUNDING

Not applicable.

CONFLICT OF INTEREST

The authors declare no conflict of interest.

EDITORIAL/PEER REVIEW

To ensure the integrity and highest quality of CytoJournal publications, the review process of this manuscript was conducted under a **double-blind model** (authors are blinded for reviewers and vice versa) through an automatic online system.

REFERENCES

1. Hanaa W, El Zeinab S, Laila R, Basma Emad A. Ticagrelor ameliorates bleomycin-induced pulmonary fibrosis in rats by the inhibition of TGF-β1/Smad3 and PI3K/AKT/mTOR pathways. Curr Mol Pharmacol 2022;15:227-38.
2. Jurgen K, David J, Andrea K. Apoptosis induction by thalidomide: Critical for limb teratogenicity but therapeutic potential in idiopathic pulmonary fibrosis? Curr Mol Pharmacol 2011;4:26-61.
3. Hu G, Huang R, Lu L, Pan Q, Chen X. Vitamin D attenuates TGF-β1-induced lung fibroblast proliferation and migration through repression of *RasGRP3*. Biocell 2023;47:1243-51.
4. Raghu G, Remy-Jardin M, Richeldi L, Thomson CC, Inoue Y, Johkoh T, *et al*. Idiopathic pulmonary fibrosis (an update) and progressive pulmonary fibrosis in adults: An official ATS/ERS/JRS/ALAT clinical practice guideline. Am J Respir Crit Care Med 2022;205:e18-47.
5. Pardo A, Selman M. The Interplay of the genetic architecture, aging, and environmental factors in the pathogenesis of idiopathic pulmonary fibrosis. Am J Respir Cell Mol Biol 2021;64:163-72.
6. Dong D, Du Y, Fei X, Yang H, Li X, Yang X, *et al*. Inflammasome activity is controlled by ZBTB16-dependent SUMOylation of ASC. Nat Commun 2023;14:8465.
7. Karagiannopoulos A, Westholm E, Ofori JK, Cowan E, Esguerra JL, Eliasson L. Glucocorticoid-mediated induction of ZBTB16 affects insulin secretion in human islets and EndoC-betaH1 beta-cells. iScience 2023;26:106555.
8. Wang K, Guo D, Yan T, Sun S, Wang Y, Zheng H, *et al*. ZBTB16 inhibits DNA replication and induces cell cycle arrest by targeting WDHD1 transcription in lung adenocarcinoma. Oncogene 2024;43:1796-810.
9. Heukels P, Moor CC, von der Thüsen JH, Wijsenbeek MS, Kool M. Inflammation and immunity in IPF pathogenesis and treatment. Respir Med 2019;147:79-91.
10. Marchioni A, Tonelli R, Cerri S, Castaniere I, Andrisani D, Gozzi F, *et al*. Pulmonary stretch and lung mechanotransduction: Implications for progression in the fibrotic lung. Int J Mol Sci 2021;22:6443.
11. Pan L, Cheng Y, Yang W, Wu X, Zhu H, Hu M, *et al*. Nintedanib ameliorates bleomycin-induced pulmonary fibrosis, inflammation, apoptosis, and oxidative stress by modulating PI3K/Akt/mTOR pathway in mice. Inflammation 2023;46:1531-42.
12. Jenkins RG, Moore BB, Chambers RC, Eickelberg O, Königshoff M, Kolb M, *et al*. An Official American Thoracic Society workshop report: Use of animal models for the preclinical assessment of potential therapies for pulmonary fibrosis. Am J Respir Cell Mol Biol 2017;56:667-79.
13. Yang W, Pan L, Cheng Y, Wu X, Huang S, Du J, *et al*. Amifostine attenuates bleomycin-induced pulmonary fibrosis in mice through inhibition of the PI3K/Akt/mTOR signaling pathway. Sci Rep 2023;13:10485.
14. Xu C, Yang C, Zhang J, Pan X, Wang J, Jiang L, *et al*. The therapeutic mechanism of dexamethasone in lung injury induced by hydrogen sulfide. Biocell 2023;47:2027-35.
15. Zhao K, Nie H, Tang Z, Chen G, Huang J. Paroxetine protects against bleomycin-induced pulmonary fibrosis by blocking GRK2/Smad3 pathway. Aging (Albany NY) 2023;15:10524-39.
16. Kropski JA, Blackwell TS. Progress in understanding and treating idiopathic pulmonary fibrosis. Annu Rev Med 2019;70:211-24.
17. Spagnolo P, Kropski JA, Jones MG, Lee JS, Rossi G, Karampitsakos T, *et al*. Idiopathic pulmonary fibrosis: Disease mechanisms and drug development. Pharmacol Ther 2021;222:107798.
18. Wei ZX, Cai XX, Fei YD, Wang Q, Hu XL, Li C, *et al*. Zbtb16 increases susceptibility of atrial fibrillation in type 2 diabetic mice via Txnip-Trx2 signaling. Cell Mol Life Sci 2024;81:88.
19. Song N, Tu H, Li Y, Xiong W, Zhang L, Liu H, *et al*. Inhibitory potential of Shen-Shuai-Ling formulation on renal interstitial fibrosis via upregulation of PLZF. Evid Based Complement Alternat Med 2022;2022:5967804.
20. Liu W, Han X, Li Q, Sun L, Wang J. Iguratimod ameliorates bleomycin-induced pulmonary fibrosis by inhibiting the EMT process and NLRP3 inflammasome activation. Biomed Pharmacother 2022;153:113460.
21. Suri GS, Kaur G, Jha CK, Tiwari M. Understanding idiopathic pulmonary fibrosis - Clinical features, molecular mechanism and therapies. Exp Gerontol 2021;153:111473.
22. Glaviano A, Foo AS, Lam HY, Yap KC, Jacot W, Jones RH, *et al*. PI3K/AKT/mTOR signaling transduction pathway and targeted therapies in cancer. Mol Cancer 2023;22:138.
23. Peng J, Xiao X, Li S, Lyu X, Gong H, Tan S, *et al*. Aspirin alleviates pulmonary fibrosis through PI3K/AKT/mTOR-mediated autophagy pathway. Exp Gerontol 2023;172:112085.
24. Li X, Ma X, Miao Y, Zhang J, Xi B, Li W, *et al*. Duvelisib attenuates bleomycin-induced pulmonary fibrosis via inhibiting the PI3K/Akt/mTOR signalling pathway. J Cell Mol Med 2023;27:422-34.

25. Zhang XL, Xing RG, Chen L, Liu CR, Miao ZG. PI3K/Akt signaling is involved in the pathogenesis of bleomycininduced pulmonary fibrosis via regulation of epithelialmesenchymal transition. Mol Med Rep 2016;14:5699-706.
26. Liu MW, Su MX, Tang DY, Hao L, Xun XH, Huang YQ. Ligustrazin increases lung cell autophagy and ameliorates paraquat-induced pulmonary fibrosis by inhibiting PI3K/Akt/mTOR and hedgehog signalling via increasing miR-193a expression. BMC Pulm Med 2019;19:35.

How to cite this article: Fang X, Wen X, Zhou L, Jiang Y, Wang L. Zinc finger and broad-complex, tramtrack, and bric-a-brac (BTB) domain containing 16 silencing attenuates bleomycin-induced pulmonary fibrosis in mice through inhibition of the phosphoinositide 3-kinase/protein kinase B/mammalian target of rapamycin pathway. CytoJournal. 2025;22:37. doi: 10.25259/Cytojournal_223_2024

HTML of this article is available FREE at:
https://dx.doi.org/10.25259/Cytojournal_223_2024